doi:10.1016/j.jmb.2007.11.070 J. Mol. Biol. (2008) 376, 153–165

JMB

Available online at www.sciencedirect.com

ScienceDirect

ELSEVIER

Threonine 429 of *Escherichia coli* σ^{70} is a Key Participant in Promoter DNA Melting by RNA Polymerase

Lisa A. Schroeder[1], Mary E. Karpen[2] and Pieter L. deHaseth[1,3]*

[1]*Center for RNA Molecular Biology, Case Western Reserve University, Cleveland, OH 44106, USA*

[2]*Chemistry Department, Grand Valley State University, Allendale, MI 49401, USA*

[3]*Department of Biochemistry, Case Western Reserve University, Cleveland, OH 44106-4973, USA*

Received 5 September 2007; received in revised form 16 November 2007; accepted 20 November 2007
Available online 21 December 2007

Edited by R. Ebright

Initiation of transcription is an important target for regulation of gene expression. In bacteria, the formation of a transcription-competent complex between RNA polymerase and a promoter involves DNA strand separation over a stretch of about 14 base pairs. Aromatic and basic residues in conserved region 2.3 of *Escherichia coli* σ^{70} had been found to participate in this process, but it is still unclear which amino acid residues initiate it. Here we report an essential role for threonine (T) at position 429 of σ^{70}: its substitution by alanine (T429A) results in the largest decrease in open complex formation yet observed for any single substitution in region 2.3. Promoter recognition itself is not affected by T429A substitution, thus providing evidence for a role of T429 in the strand-separation step. Our data are consistent with a model where the T429 would act as a competitor for the hydrogen bonding that stabilizes the highly conserved −11A-T base pairs of the promoter DNA, thus facilitating initiation of strand separation at this particular position in the −10 region. This model suggests an active role for RNA polymerase in disrupting the −11 base pair, rather than just capturing the −11A subsequent to spontaneous unpairing.

Keywords: RNA polymerase; sigma factor; promoter; strand separation

Introduction

Sigma factors constitute a class of bacterial transcription factors that bind to the RNA polymerase (RNAP) "core enzyme" E to form "holoenzyme" Eσ. In this complex, the sigma factor functions in the sequence-specific recognition of promoter DNA and plays an essential role in the promoter DNA-strand-separation step required for initiation of transcription. *Escherichia coli* has seven different sigma factors, including σ^{70}, which is required for transcription of housekeeping genes. Four regions of sequence conservation, some of which are further divided into subregions, have been recognized. Region 2.3, consisting of 18 amino acids, is the DNA melting region of σ^{70}.[1,2]

It is thought that promoter DNA melting is initiated in the −10 region, consensus sequence TATAAT, at the highly conserved A-T base pair, which is located at position −11 (underlined) in most promoters by a mechanism involving rotation ("flipping") of A out of the DNA helix and into a pocket on RNAP.[3] Once that has occurred, strand separation would propagate downstream to about position +3, just past the start site of transcription, to form the open complex. This is a complicated process involving conformational changes in RNAP. The extensive work of Craig *et al.*, Saecker *et al.*, and Davis *et al.* on open complex formation at the λ P_R promoter has established the occurrence of two intermediates, in addition to the first specific (closed) complex.[4–6] This would lead to the following scheme:[1] $R + P \leftrightarrow RP_c \leftrightarrow I_1 \leftrightarrow I_2 \leftrightarrow RP_o$. Both RP_c and I_1 are sensitive to the competitor, heparin, while I_2 and RP_o are competitor resistant.[4] The promoter region covered by RNAP is smaller in RP_c, extending downstream to about +1, than in I_1, I_2, and RP_o, reaching about +20.[4]

**Corresponding author.* Center for RNA Molecular Biology, Case Western Reserve University, Cleveland, OH 44106, USA. E-mail address: pld2@case.edu.

Abbreviations used: RNAP, RNA polymerase; WT, wild type; EMSA, electrophoretic mobility shift assay; FBB, fork-binding buffer; EDTA, ethylenediaminetetraacetic acid.

Much work has been devoted to the study of the mechanism of DNA melting by bacterial RNAP; however, to date, it is not yet clear how the process is initiated. Several amino acids in region 2.3 of σ^{70} had previously been identified as playing a role in this process,[3,7–10] but amino acid residues that have been proven to interact with the −11A-T base pair of promoter DNA during the formation of the open complex have yet to be identified. Our recent studies called in question whether the region 2.3 residues Y430 and W433, which have been previously thought to interact with −11A, are indeed its likely interacting partners.[11] Some time ago, a study by Waldburger and Susskind identified a threonine at position 429 of σ^{70} as being uniquely important, as no substitution other than serine was found to result in significant promoter activity *in vivo*.[12] This would be indicative of an essential role for the hydroxyl group that threonine and serine have in common. The experiments reported here demonstrate that T429A substitution in σ^{70} impedes open complex formation to a greater extent than any other single substitution in σ^{70}. We postulate that T429 may play an essential role in disrupting the −11A-T base pair as a prelude to flipping the 11A out of the helix.

Results

T429A substitution greatly impedes stable RNAP–promoter complex formation

In our effort to identify amino acid residues of σ^{70} that are important in the early stages of the RNAP-induced strand-separation process, we introduced substitutions at T429 and T432. We chose these amino acids, which are capable of H-bonding, in view of the proposal of Matlock and Heyduk that amino acid residues of σ^{70} might nucleate promoter DNA melting by competing with the H-bonding stabilizing the −11A-T base pair.[13] In addition, T429 had previously been found to be of critical importance[12] (see earlier discussion). Our data indicated that while T432A substitution had effects that were qualitatively similar to those of Y430A and W433A (e.g., Schroeder *et al.* [11]), the T429A substitution was more deleterious than observed for any other single substitution tested in region 2.3 (data not shown).

To explore the DNA target of T429, we used promoter DNAs bearing abasic sites, as shown in Fig. 1a. Abasic sites are useful in assessing whether a particular amino acid substitution affects either interactions with the missing base or base pairing involving this base; here, they help elucidate the latter (as discussed later). Prior to gel analysis, the complexes were challenged by the competitor, heparin, to ensure that only stable RNAP–promoter complexes were considered. The results, obtained at room temperature (23–26 °C), reveal the large negative effect of the T429A substitution on the interaction with short duplex DNA. A similar negative effect of the T429A substitution is seen with DNA bearing a −11 abasic site in the top (nontemplate) strand; however, with this template, complex formation with wild-type (WT) RNAP is reduced as well, when compared to that of the short duplex DNA with WT RNAP. These results underscore the importance of both T429 and −11A in stable complex formation (see Fig. 1b and c).

If the abasic site is on the template strand (−11 Ab D Bot), a slight increase in the extent of stable complex formation is seen for the WT, but a much greater increase is seen for the T429A RNAP. With −11A already unpaired due to the absence of its base-pairing partner on the template strand, T429 may no longer be critical. Abasic sites at position −10 also greatly facilitate complex formation, but the differences between the binding of promoters with the abasic sites on the template strand and the binding of promoters with the abasic sites on the nontemplate strand are not as pronounced. In either case, the weakening of the base pairing due to the abasic sites must be more important than any other interactions that might have been disrupted due to the missing bases. Abasic sites at position −12 have smaller effects. The base pair at −12 is not normally melted in the open complex; thus, any effects of abasic sites here might be due to their effects on the base pairing at −11.[14] The −11 and −10 abasic sites in the template DNA restore complex formation by RNAP with the T429A substitution to similarly large extents, suggesting that T429 may function in disrupting either the −11 or the −10 base pairs.

We also carried out experiments with short duplex DNA and −10 and −11 abasic bottom (see Fig. 1a) where the concentrations of RNAP and promoter DNA had been reduced by fivefold to 10 nM RNAP and 2 nM DNA, respectively. All binding percentages were lower as a result (data not shown), indicating that binding was not performed at saturation, which would have resulted in loss of the ability to fully detect increases in binding affinity. These results confirm that the presence of the abasic site at −11 of the template strand improves binding affinity for T429A RNAP to a much greater extent than for WT RNAP. A similar difference is observed when comparing the effects of the −10 abasic site in the template strand. The observation that the effect of the template strand abasic site is to preferentially rescue the defect of the T429A substitution is consistent with a role of T429 in disrupting the −11 and/or the −10 base pairing (see Discussion).

T429A substitution does not affect DNA binding by RNAP

The T429A substitution may lead to a defect in stable complex formation due to an impaired ability to bind to promoter DNA in a closed complex under the conditions of the experiments shown in Fig. 1. To address this possibility, we carried out the electrophoretic mobility shift assay (EMSA) experiments shown in Fig. 1d. RNAP and short duplex DNA were incubated exactly as for the experiments shown in Fig. 1b and c, but without heparin

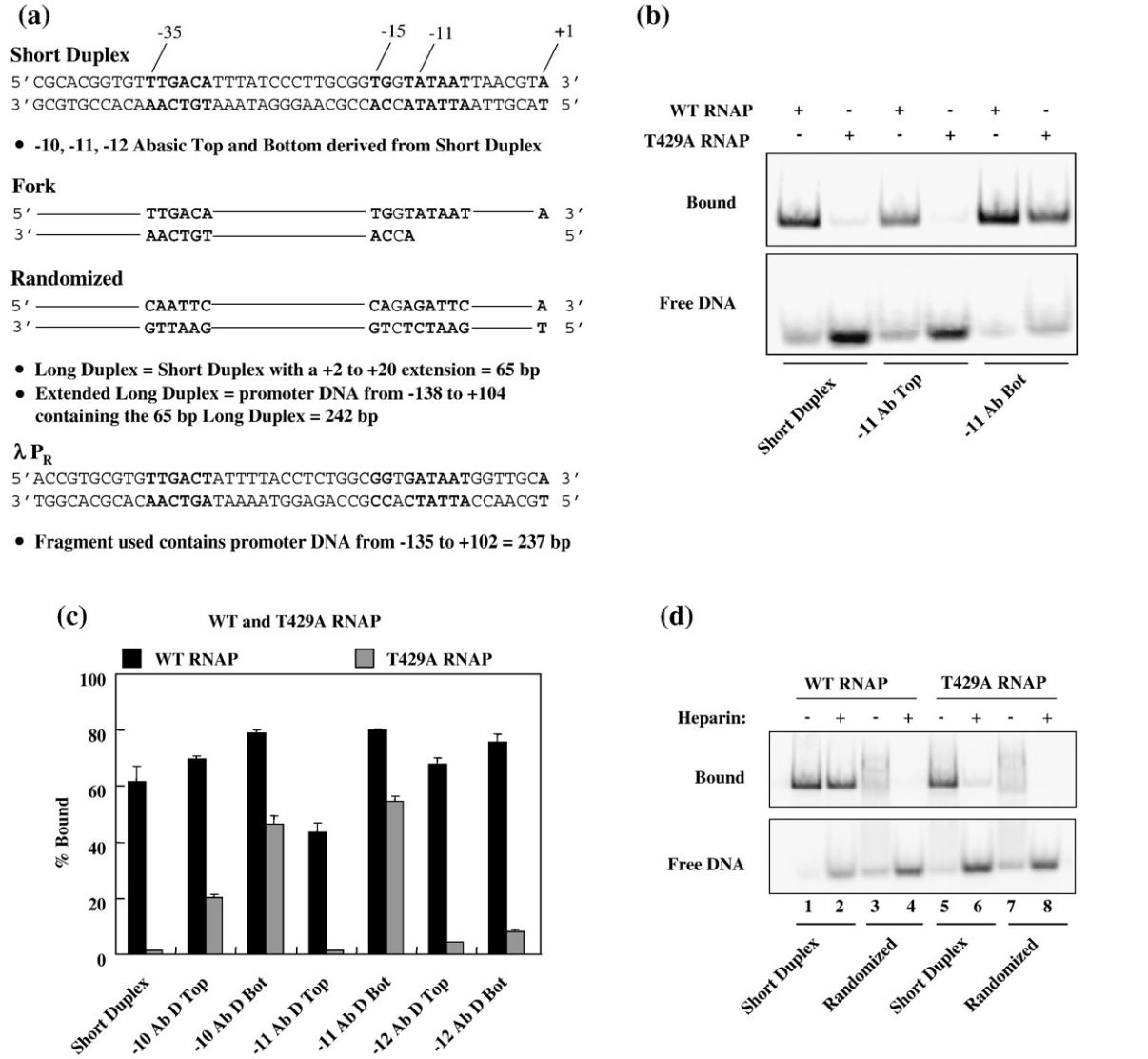

Fig. 1. The T429A substitution is highly deleterious to open, but not closed, complex formation. (a) DNA templates used in this work. The consensus −35, extended −10, and −10 promoter elements are shown in bold, as is the transcription start site. The promoter in the randomized DNA has been inactivated by base substitutions. (b) The effects of the T429A substitution in σ^{70} on the ability of holoenzymes to form heparin-resistant complexes with the DNA templates indicated at room temperature: EMSA gel. Only the regions of the gel containing the free and RNAP-bound DNA are shown. Ab = Abasic. (c) Quantification of the extents of binding determined by EMSA gels such as that shown in (b). D = duplex; Bot = bottom strand. (d) RNAP was incubated for 10 min at room temperature with either short duplex DNA or randomized DNA. The mixtures were analyzed by EMSA, both with and without prior heparin challenge. Only the regions of the gel containing the free and RNAP-bound DNA are shown.

challenge, and the mixtures were subjected to electrophoresis on a nondenaturing gel. A comparison of lanes 1 and 5 indicates that, under these conditions, WT and T429A RNAP show very similar extents of complex formation (99% and 95%, respectively). Additionally, heparin-sensitive complexes are observed to form within 30 s of the mixing of both WT and T429A (data not shown). In agreement with the results displayed in Fig. 1c (first two bars), it was found that, during the 10-min incubation, most of the complexes formed with WT RNAP were heparin resistant (lane 2), but that very few complexes formed with the T429A RNAP were heparin resistant (lane 6).

To assess whether the complexes formed in the absence of heparin are specific, we also used a short duplex DNA carrying a randomized sequence, instead of the promoter (randomized in Fig. 1a). It is seen in lanes 3 and 7 of Fig. 1d that the complexes formed with this DNA have diffuse bands, in contrast to the sharp bands observed with short duplex DNA (lanes 1 and 5). The diffuse bands obtained with the randomized DNA may be due to nonspecific binding of RNAP at different locations, leading to a range of mobilities of the complexes. As expected, the complexes formed with the randomized DNA and both WT and T429A RNAP are heparin sensitive. In aggregate, these results in-

dicate that the T429A substitution does not lead to defects in promoter recognition and closed complex formation.

σ70 with T429A substitution can bind core RNAP

We had previously concluded from gel-shift analysis of reconstitution reactions containing both σ^{70} and the core enzyme that the T429A substitution affected the interaction of σ^{70} with the core enzyme.[10] However, inspection of this work revealed anomalies in the gel pattern: while formation of the holoenzyme was not detectable, neither was the band representing free core RNAP, casting doubt on our earlier interpretation of the results. The bands on the gel of Fig. 2a demonstrate that the earlier conclusion was incorrect. Upon repeat of the experiment, as described in Materials and Methods, with

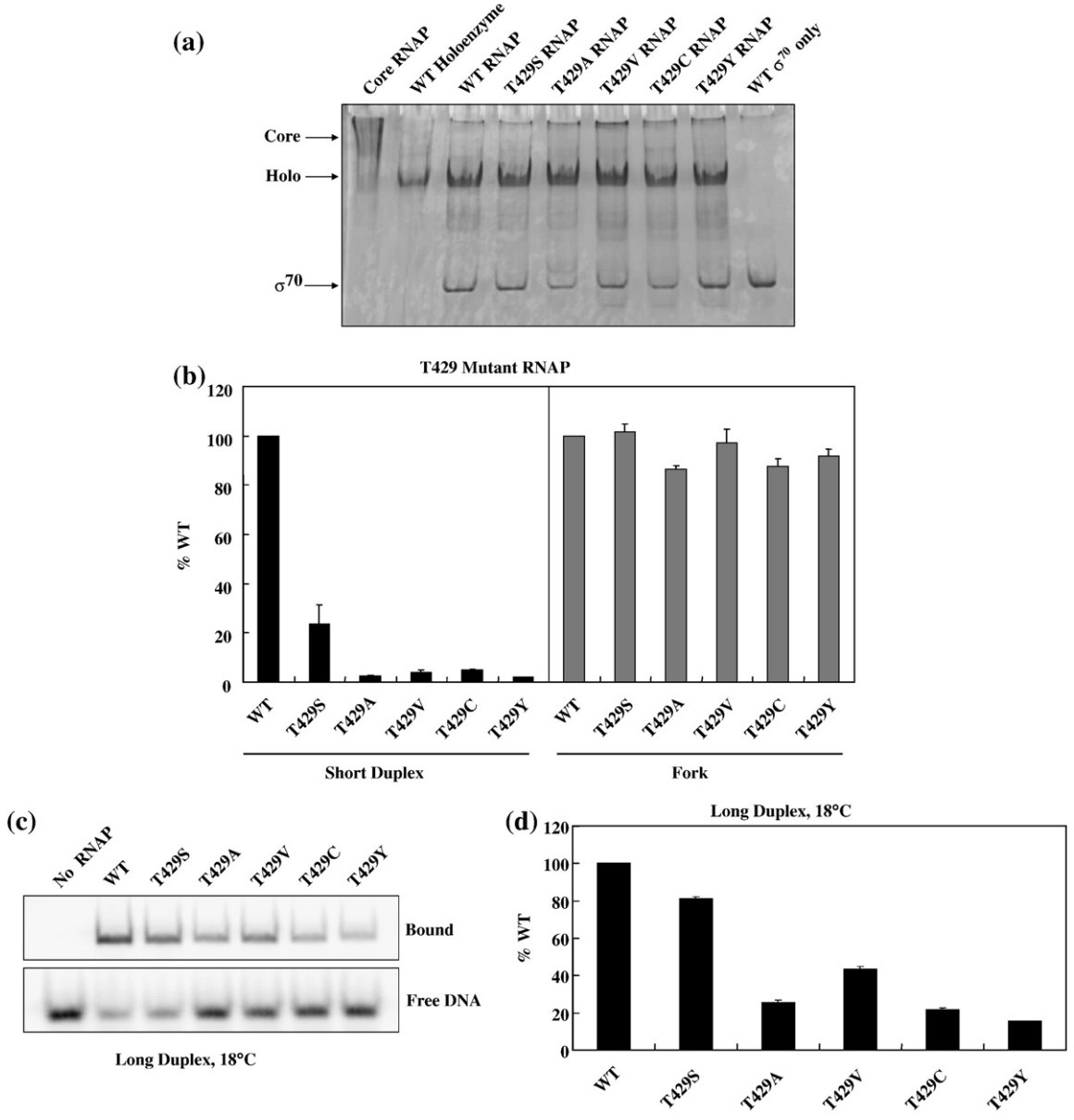

Fig. 2. Comparison of the effects of various substitutions for residue 429 of σ^{70} on the formation of the holoenzyme and stable complexes at promoters. (a) Determination of the ability of the σ^{70} substituted at position 429 to interact with the RNAP core enzyme. Bands due to the holoenzyme (holo) and free σ^{70} are indicated. The lane labeled WT Holoenzyme contains RNAP that was purified as the holoenzyme, as opposed to holo-RNAP reconstituted from sigma factor and core RNAP. (b) Effects of T429 mutant RNAP on the interaction with short duplex DNA and fork DNA, as determined by EMSA analysis of heparin-challenged binding reactions carried out at room temperature. For each template, the data were normalized to that obtained with WT RNAP. (c) Representative EMSA gel for determining the effects of various substitutions for the T429 on the formation of heparin-stable complexes between RNAP and the long duplex DNA at 18 °C. RNAP and DNA were incubated for 5 min at 18 °C, followed by heparin challenge for 5 min. The EMSA gel was run at 18 °C as well. Only the regions of the gel containing the free and RNAP-bound DNA are shown. (d) Quantification of gels such as that shown in (c). Values were normalized to that obtained with WT RNAP.

σ^{70} bearing the T429A, as well as four other single substitutions, it is evident that each is able to bind the core enzyme equally well as WT σ^{70} to form the holoenzyme. The results reveal essentially complete disappearance of the core band, with concomitant appearance of a new band corresponding to the holoenzyme. A duplicate gel (not shown) displayed the same pattern. Addition of a greater excess of σ^{70} over core RNAP in the reconstitution reaction did not rescue the low percentage of heparin-resistant complexes seen with T429A RNAP and short duplex DNA (data not shown), providing further indication that, under our experimental conditions, the T429A substitution does not impair the σ^{70}–core interaction.

A side chain bearing a hydroxyl group is essential at position 429 of σ^{70}

The results of experiments on the interaction of the short duplex DNA template (see first six bars in Fig. 2b) with the holoenzyme containing WT σ^{70} and σ^{70} bearing five different substitutions at 429 indicate that, with this DNA, the only substitution that allows significant DNA-binding activity is T429S. Interestingly, when a fork-junction template is used where −11A is unpaired (Fig. 1a), all variants showed similar extents of complex formation (next six bars in Fig. 2b), suggesting that T429 may participate in disrupting the −11A-T base pair, so that a substitution for T429 would have no effect if −11A is already unpaired.

To better differentiate among the effects of the substitutions for T429, we also studied binding to long duplex DNA[15] (see Fig. 1a), a full-length promoter and, as such, more physiologically relevant. However, with this promoter, the extent of stable complex formation at room temperature is increased, such that the difference between WT and T429A RNAP is partially obscured. Therefore, the effects of various substitutions for T429 on heparin-resistant complex formation with long duplex DNA were compared at the reduced temperature of 18 °C (see Fig. 2c for a representative gel; see Fig. 2d for a quantitative representation). The serine (i.e., T429S) allowed, by far, the greatest extent of formation of a stable heparin-resistant complex among the substitutions tested, consistent with the *in vivo* transcription results from Waldburger and Susskind and with the results shown in Fig. 2b.[12] Thus, the hydroxyl group, shared by T and S, must be essential for the formation of a stable complex, while the tyrosine (T429Y) side chain would be too large to properly present its hydroxyl group and may experience steric hindrance. The cysteine (T429C) showed a low extent of binding, considerably less than that of the serine, in keeping with the fact that the sulfhydryl group is worse at hydrogen bonding than the hydroxyl. Valine (T429V) is similar in size to threonine and also has a methyl group, but lacks the hydroxyl group. It allows less promoter DNA binding in a stable complex than serine, but more than the other substitutions tested. Very similar results were also obtained at room temperature with long duplex DNA, bearing a 2-AP substitution for −11A in the nontemplate strand, which is known to mitigate open complex formation.[11,14,16,17] As a consequence, the 2-AP-substituted promoter also allows good differentiation among RNAPs bearing various amino acid substitutions in region 2.3 of σ^{70}, according to their abilities to carry out DNA strand separation.

T429A decreases the rate of stable complex formation with promoter DNA

The mechanism whereby the T429A substitution leads to the formation of fewer stable promoter complexes was probed by an investigation of the kinetics of the formation and dissociation of stable complexes for WT and T429A RNAP with the long duplex DNA at 18 °C. Sample results for the association kinetics obtained by quantification of the stable complex band for each time point in gels such as that shown in Fig. 3a are displayed in Fig. 3b and summarized in Table 1. The association rate constants for stable complex formation by WT and W433A RNAP are seen to be very similar and twice as large as that for Y430A RNAP, which in turn is four to five times larger than that for T429A RNAP. On the other hand, the amplitudes are all very similar. Eventually, even the T429A RNAP will form open complexes at 80% of the promoters. Experiments carried out at room temperature with long duplex DNA bearing the −11 2-AP substitution lead to a similar conclusion (data not shown).

No decay of the "stable" complexes containing either WT or T429A RNAP was detectable over a time scale of 60 min (data not shown), precluding determinations of a dissociation rate constant. Because the complexes are so stable, it is quite possible that the effects of the T429A substitution on the stability of the RNAP–promoter complexes may have remained undetected. Complexes of RNAP with short duplex DNA are considerably less stable,[11] but that template could not be used here with T429A for either association or dissociation experiments, in view of the very low extents of binding obtained (e.g., see Fig. 1c). Thus, it is difficult to compare the current results with those obtained previously for complexes of RNAP containing substitutions at Y430 and W433[11] with short duplex DNA. With the latter DNA, no effects of Y430 and W433 substitutions on the association kinetics were observed, but the complex half life was found to be a factor of 2 less than that observed with WT RNAP.

T429A substitution slows, but does not prevent, promoter DNA melting

To directly determine the effect of the T429A substitution in σ^{70} on RNAP-dependent promoter DNA melting, we carried out $KMnO_4$ probing experiments to monitor DNA strand opening. The T's in single-stranded regions of DNA are oxidized

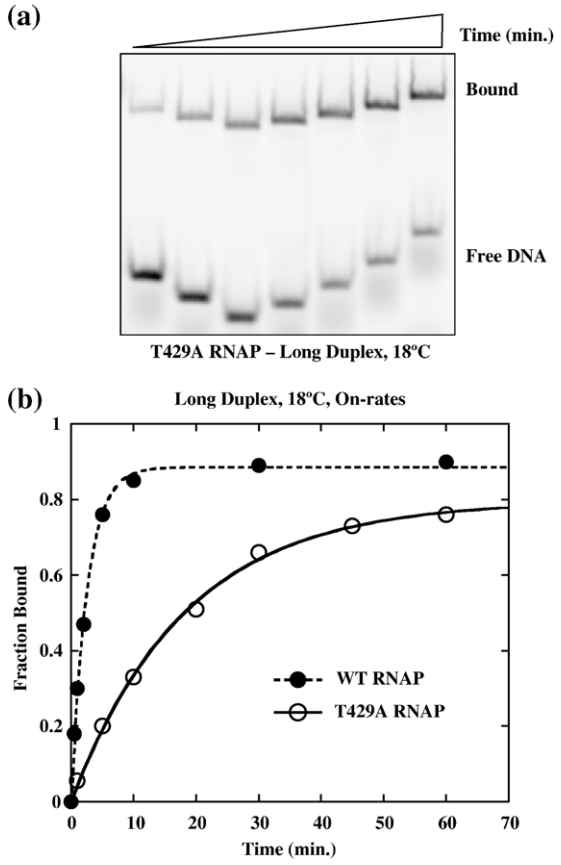

Fig. 3. The T429A substitution in σ^{70} slows the kinetics of stable complex formation between RNAP and long duplex promoter DNA at 18 °C. (a) A representative EMSA gel showing the increased formation of heparin-stable complexes of T429A and long duplex DNA over time at 18 °C. The samples were incubated individually and run on the gel for different amounts of time, causing the observed differences in the migration of free DNA and complexes. (b) A plot of the fraction of stable complexes *versus* time for WT and T429A RNAP. The circles represent the data points, and the lines represent the single-exponential fits to the points. The average parameters for the fits to duplicate sets of data are shown in Table 1.

by $KMnO_4$, thus rendering the DNA sensitive to piperidine-induced cleavage. In Fig. 4, the results of such an experiment with long duplex DNA at 18 °C are shown. The samples where the promoter DNA was incubated with WT RNAP for 10 min or 60 min prior to probing with $KMnO_4$ showed prominent bands (Fig. 4a) indicative of extensive strand separation. The data have been quantified and are shown in Fig. 4b as percentages of the extent of melting seen with WT RNAP after a 60-min incubation with the promoter DNA. With T429A RNAP, strand separation is slow, consistent with the observed kinetics (Fig. 3); however, at 60 min, a significant extent of melting could be observed. For Y430 and W433 RNAP, the extents of DNA melting are very similar to those seen for WT RNAP (data not shown). For reactions containing 50 nM RNAP and 10 nM promoter DNA incubated for 10 min, it is expected that most of the DNA will be bound by RNAP containing WT, T429A, Y430A, and W433A σ^{70} (see Fig. 1d), so that the results described here reflect a pronounced defect in the ability of the T429A RNAP to melt promoter DNA. Consistent with expectations, the nonmelting FYWW RNAP[18,19] did not show any detectable melting of −11 2-AP-substituted long duplex DNA, even after an hour of incubation at room temperature and a concentration of 200 nM, which would result in most of the FYWW RNAP being bound by the promoter DNA[19] (data not shown).

T429A substitution exerts its effects at a step after closed complex formation

In order to try and pinpoint at what step in the kinetic scheme the consequences of the T429A substitution manifest themselves, we carried out DNase I footprinting on the extended long duplex, a promoter with the sequence of the long duplex DNA but in the context of a longer DNA fragment, which is necessary to obtain good footprinting patterns (see Fig. 1a for DNA sequences; see Fig. 5a and b for footprinting). To be able to capture the closed complex, we used short incubation times (0.5 min) and low temperature (9 °C). Incubation of the extended long duplex for 0.5 min with WT RNAP (or Y430A and W433A RNAP; data not shown) or for 10 min with T429A RNAP led to a long heparin-resistant DNase I footprint, stretching from about −44 to +25, characteristic of an open complex. However, a 0.5-min incubation of extended long duplex with T429A RNAP resulted mainly in a shorter heparin-sensitive footprint, extending from approximately −44 to about +5, characteristic of a closed complex.

This assignment is further supported by probing the above complexes with $KMnO_4$ in order to directly monitor RNAP-induced strand opening. Indeed, $KMnO_4$ probing of the complexes exhibiting a long footprint indicated that strand separation had occurred, as deduced by DNA strand breakage at +2T/−1T, −6T, and −10T in the nontemplate strand (see Fig. 5c). However, much fainter bands can be seen for the complexes with short footprints, formed after a 0.5-min incubation of the extended long duplex with T429A RNAP. From band intensities, it

Table 1. The effects of alanine substitutions for various RNAPs on the kinetics of stable complex formation with the long duplex promoter at 18 °C

RNAP[a]	A[b]	k_{obs} (min^{-1})[c]
WT	0.90±0.0	0.40±0.01
T429A	0.80±0.01	0.05±0.00
Y430A	0.88±0.01	0.23±0.01
W433A	0.91±0.01	0.39±0.03

[a] In all cases, the concentration of RNAP was 50 nM and that of DNA was 10 nM.
[b] A is the amplitude of the reaction in the fraction of total DNA in the stable complex.
[c] k_{obs} is the pseudo-first-order rate constant.

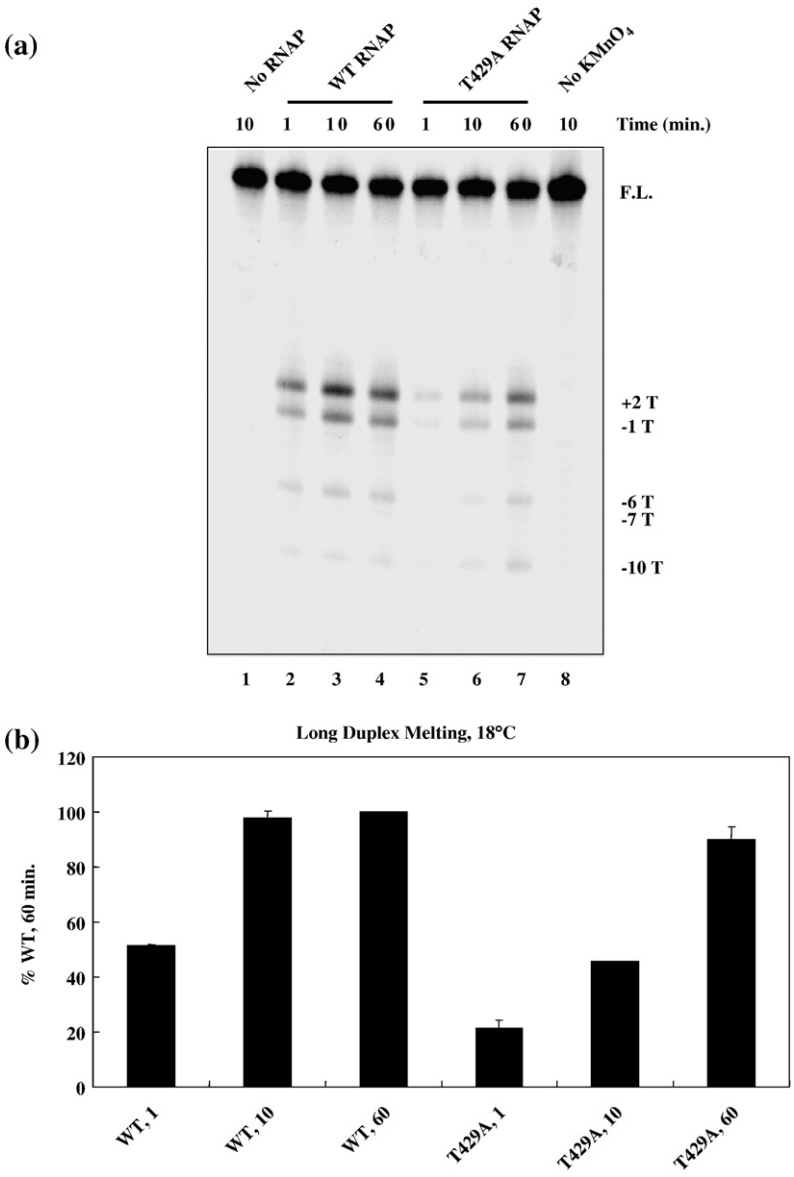

Fig. 4. $KMnO_4$ probing of T429A RNAP and long duplex DNA complexes reveals slow melting of the promoter compared to WT RNAP at 18 °C. (a) Representative 8% $KMnO_4$ footprinting gel. The time is the length of incubation of radiolabeled DNA and RNAP before $KMnO_4$ is added. FL = full-length DNA at 65 bases. Bands representing oxidation of −10T, −7T, −6T, −1T, and +2T are marked. The nontemplate strand of the long duplex DNA was 5′ end labeled with ^{33}P. (b) Quantification of the data from gels such as that shown in (a). Values are expressed as the percentages of melting of the −1 and +2T bands divided by the band for the full-length DNA (see Materials and Methods), and then normalized to WT RNAP value after a 60-min incubation. The numbers after RNAP on the *x*-axis represent the time of incubation (in minutes).

can be calculated that these conditions lead to the melting of approximately 26% of the DNA as compared to WT RNAP, in agreement with the 26% estimated from EMSA analysis of heparin-challenged binding reactions carried out under the same conditions as the DNase I footprinting (data not shown). The two prominent bands downstream of the presumed closed complex boundary are each about 50% protected from DNase I cleavage (see Fig. 5b). Some of this protection is due to the open complexes formed at 26% of the promoters during the 0.5-min incubation with T429A RNAP. Some or all of the remaining 20–30% protection may be due to I_1, consistent with our observation that there likely is both heparin-resistant and heparin-sensitive protection of the above two bands (data not shown). For this strong promoter, the I_1-to-I_2 conversion is expected to be very fast; thus, such accumulation of I_1 would be indicative of an effect of the T429A substitution on the I_1-to-I_2 conversion as well. Technical reasons (heparin sensitivity of the DNase I cleavage reaction itself) precluded more precise quantification of the extent of heparin-sensitive protection of the DNA.

We also footprinted the complexes formed by T429A RNAP and the well-studied λ P_R promoter DNA [see Fig. 6a (gel) and Fig. 6b (traces)]. Closed complexes show a short footprint at this promoter[10] as well, and also at a variant of the P_R promoter bearing a G-12T substitution,[19] while for I_1, I_2, and RP_o complexes, a footprint extended in the downstream direction is observed.[4,5] With WT RNAP, after a 10-min incubation at room temperature, essentially all the DNA is protected over a region extending to +20 (lane 2) in a complex that survives heparin challenge (lane 3), consistent with an open complex. On the P_R promoter, which is weaker than the extended long duplex, after a 10-min incubation of the DNA and T429A RNAP, a short (lane 4) and heparin-sensitive (lane 5) footprint is observed, characteristic of the closed complex. The traces of the gel shown in Fig. 6a are presented in Fig. 6b,

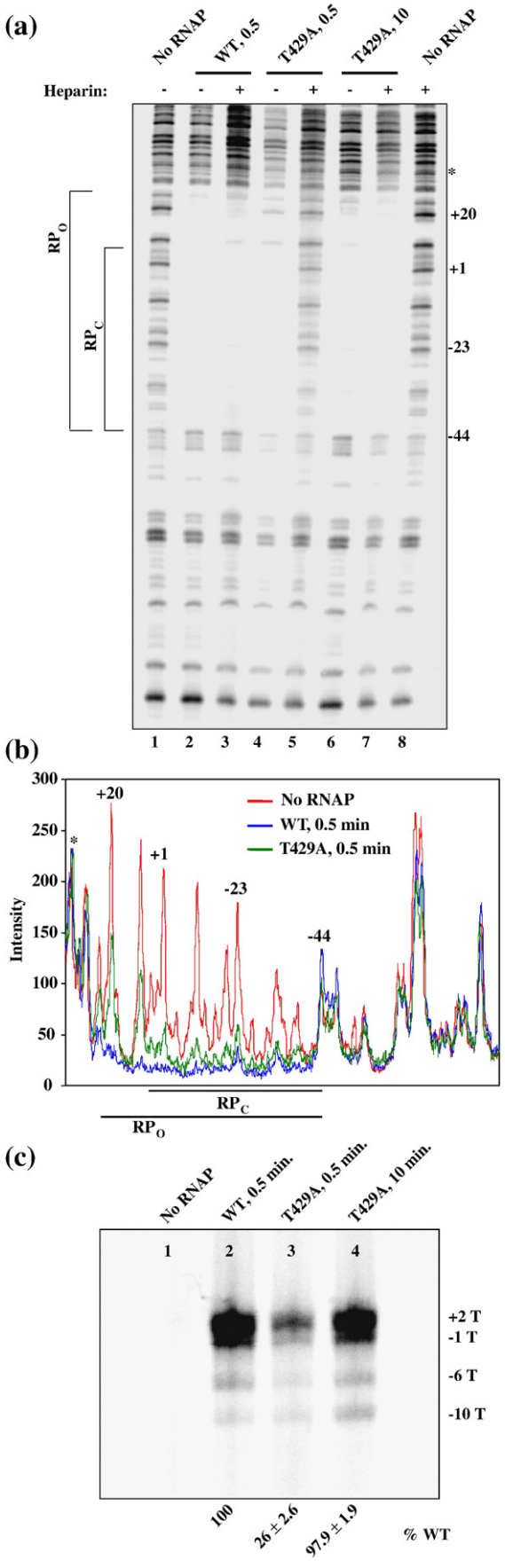

which clearly displays the differences between the long and the short footprints. The results are in good agreement with those obtained before,[19] not only with respect to the footprints for WT RNAP but also in comparing the short footprints for T429A RNAP with those seen earlier for FYWW RNAP. Thus, the T429A substitution causes an accumulation of RP_C, consistent with a defect of T429A RNAP in carrying out the RP_C-to-I_1 step. In contrast to the results obtained for the extended long duplex, there is little additional protection of DNA downstream of the presumed closed complex boundary for the T429A RNAP, obviating the need for invoking the effects of the T429A substitution at steps beyond the RP_c-to-I_1 transition.

Discussion

We have established the exquisite importance of the σ^{70} T429 residue in the formation of a stable strand-separated RNAP–promoter complex by demonstrating that the T429A substitution is highly deleterious to this process. Several lines of evidence are consistent with T429 being involved in promoter DNA strand separation. First, as is shown by the results presented in Fig. 1d, the T429A substitution does not affect closed complex formation, indicating that subsequent steps involved in the nucleation of promoter DNA melting are affected. Second, the effects of the T429A substitution are mitigated if

Fig. 5. The T429A substitution exerts its effects at a step beyond the formation of the closed complex. (a) DNase I footprinting of RNAP complexes at the extended long duplex promoter. Image of the radioactive bands of single-stranded DNA fragments on a 6% denaturing gel. The 5′ end of the nontemplate strand is radiolabeled. The area of the footprint representing the closed and open complexes is marked. Band positions (within one- to two-base accuracy) were identified by DNA sequencing (Sequenase Version 2.0 PCR Product Sequencing Kit, USB). The band marked with an asterisk was used for normalization in (b). The numbers after RNAP represent the time of incubation (in minutes) of RNAP and promoter DNA prior to addition of heparin, where indicated, and DNase I. (b) Scan of individual lanes of the gel shown earlier as (a). The scans shown (all without heparin addition) represent lane 1 (No RNAP), lane 2 (WT RNAP, 0.5 min of incubation), and lane 4 (T429A RNAP, 0.5 min of incubation). The asterisk represents the band used for the peak normalization of the No-RNAP reaction. Band positions and the closed and open complex boundaries are assigned as represented in the gel for (a). (c) RNAP-induced strand opening at the extended long duplex promoter. $KMnO_4$ modifications of thymine residues that become single stranded (band positions denoted on the right side of the gel) are compared in the presence of heparin without RNAP (lane 1), with a 0.5-min incubation with WT RNAP (lane 2) and T429A RNAP (lane 3), and with a 10-min incubation with T429A RNAP (lane 4). The percentage of promoter DNA melting (determined as described in Materials and Methods), normalized to that for WT RNAP reaction incubated for 0.5 min, is shown below the lane for each reaction with RNAP.

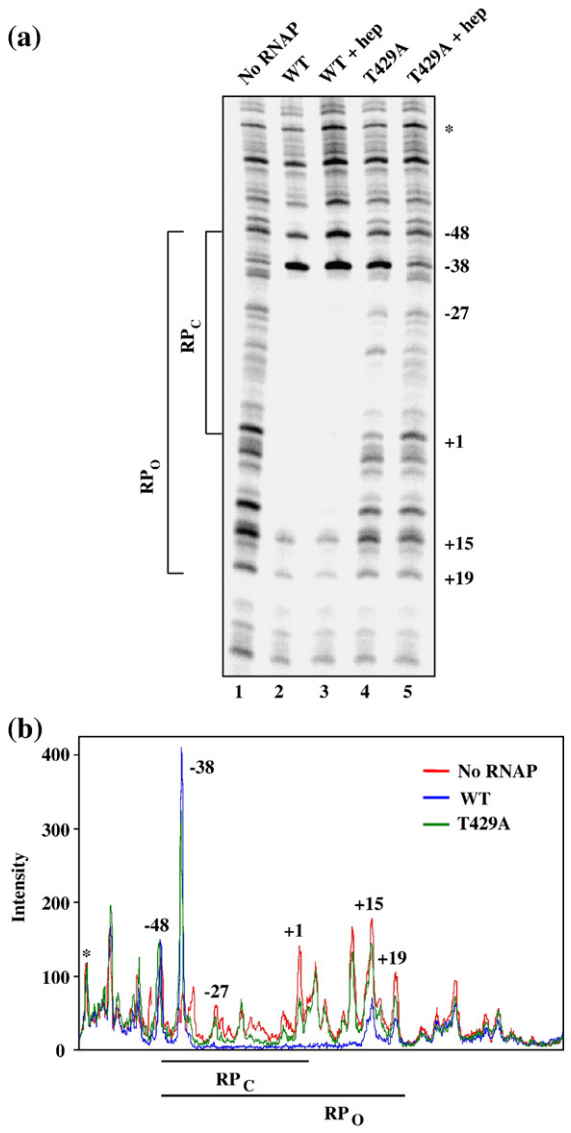

Fig. 6. DNase I footprinting on the λ P_R promoter reveals that a significant fraction of T429A RNAP–DNA complexes for this promoter comprises closed complexes. (a) A 6% denaturing gel of the bands due to cutting by DNase I in the presence of RNAP and the 237-bp λ P_R promoter DNA. The 5′ end of the template strand is labeled with ^{33}P. The short footprint representing closed complex formation is labeled RP_c, and the long footprint is labeled RP_o. Bands representing DNA of a certain length are marked, and the asterisk denotes the band used for normalization in (b). (b) Scan of individual lanes of the gel represented earlier as (a). The scans shown (all without heparin addition and at 10 min of incubation) correspond to lane 1 (No RNAP), lane 2 (WT RNAP), and lane 4 (T429A RNAP) of (a). The asterisk represents the band used for the peak normalization of the No-RNAP reaction. Band positions and the closed and open complex boundaries are assigned as represented in the gel for (a). As described in Materials and Methods, the traces for No RNAP and T429A RNAP were adjusted in this scan in order to properly align the peaks due to slightly uneven running of the lanes of the gel shown in (a).

−11A (or −10T) is already unpaired, as is the case for both fork DNA and promoter DNA with an abasic site in the template strand, but not (or to a much smaller extent) in the nontemplate strand (see Figs. 1c and 2b). That the level of abasic promoter DNA binding is not completely restored to that seen with WT RNAP points to T429's likely involvement in interactions other than that necessary for strand separation of the −11A-T base pair (as discussed later). Third, the T429A substitution slows the kinetics of formation of the stable promoter complex (see Figs. 3 and 4). Finally, by DNase I footprinting (Fig. 5a and b; Fig. 6a and b), we were able to detect an accumulation of the closed complex. Our data are consistent with an effect of the T429A substitution on the RP_c-to-I_1 step. However, as pointed out earlier (see Results and Fig. 5b), for the extended long duplex, we cannot conclusively rule out an accumulation of an I_1-like intermediate and an (additional) effect of the T429A substitution on the I_1-to-I_2 conversion. No such additional inhibition needs to be invoked for the P_R promoter.

Proposed mechanism of action for T429

The evidence presented earlier strongly supports a role for T429 in the nucleation of the strand separation of promoter DNA. A large body of data indicates that initiation of DNA melting occurs at the −11A-T base pair.[3,11,13,14,16,20–22] Taken together, this would suggest that an important target for T429 is the A-T base pair at −11. However, the data in Fig. 1c indicate that the effects of abasic sites at −10 on either strand of promoter DNA are large as well. There are several possible explanations for this observation. The abasic sites at −10 may facilitate initiation of DNA melting at this position and/or exert an indirect effect by decreasing the stability of the −11 base pair. However, the possibility that T429 also interacts with the −10 base pair cannot be ruled out. Interestingly, the data displayed in Figs. 4a and 5c show that WT RNAP protects −10T from $KMnO_4$ oxidation to a greater extent (relative to −6T) than T429A RNAP, supporting the proximity of T429 and −10T during at least some phase of open complex formation. Thus, all four bases participating in base pairing at −11 and −10 need to be considered as possible targets of T429.

In order to determine the feasibility of base-pair disruption through H-bonding to the hydroxyl of T429, we focused on the area surrounding the T429, using the 6.5-Å structure obtained by Murakami *et al.*[23] This structure is a complex of *E. coli* holoenzyme with a fork-junction DNA template similar to the fork DNA used in this work, which would likely represent an open complex. Ideally, we would use a closed complex or other intermediate complex structure for modeling, but these have not yet been solved. Using the coordinates of this "open" complex structure, we have constructed the model presented in Fig. 7 (see Materials and Methods), which shows that the bases at −11 and −10 of the nontemplate strand are within 9 Å of T429. As T429

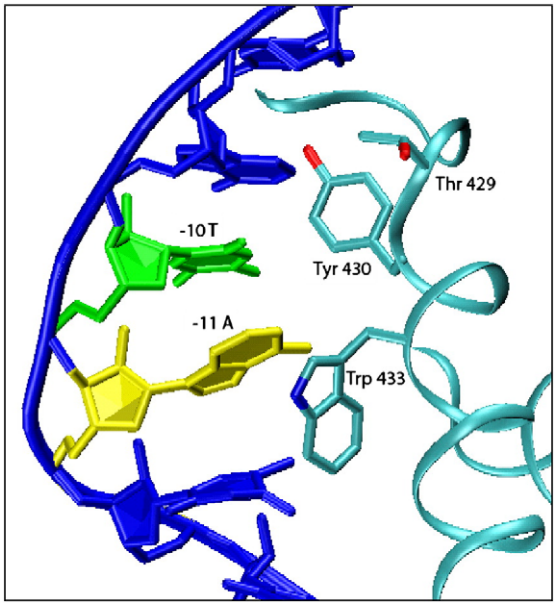

Fig. 7. T429 is in the vicinity of the −10 region. A model of the −10/−11 binding pocket in the RNAP holoenzyme open complex (adapted from Protein Data Bank file 1L9Z[23]) showing that, in the open complex, T429 is positioned in proximity to the −10 region of the nontemplate strand. A portion of σ^{70} is rendered in cyan. The side chains of T429 (252), Y430 (253), and W433 (256) are shown (the *T. aquaticus* numbering is given in parentheses). The nontemplate DNA strand is shown in dark blue, with the −11 base shown in yellow and the −10 base shown in green.

exerts its effect at an early stage during open complex formation (Figs. 5 and 6), it is likely that a subsequent conformational change may have occurred during this process, which would have moved the T429 out of H-bonding distance (3 Å) from the −11 and/or the −10) base pairs—its likely targets. Residues Y430 and W433, also shown to be in close proximity to the −10 region (Fig. 7), play important, albeit not critical, roles in open complex formation.[8–10]

Support for conformational changes during open complex formation is derived from the modeling of the template strand downstream of −12 as forming a B-helix with the nontemplate strand, to emulate a closed complex (model not shown). This strand would clash with amino acids in region 2.3 of σ^{70}, including the T429; thus, this region of σ^{70} must have been repositioned subsequent to strand separation and insertion of the template strand into the tunnel leading to the active site of RNAP. Additional support comes from the observation that Q437 and T440, both of which have been shown to interact with the −12T base,[24] are also outside the H-bonding range to this base. Thus, conformational changes in the pathway from the closed complex to the open complex likely positioned the amino acid and base interacting partners so they could no longer interact. In conclusion, the modeling demonstrates not only that T429 is on the surface of the sigma subunit and able to contact the nontemplate strand but also that only a small adjustment in distance would suffice for the T429 to be able to interact with the −11 or the −10 base region.

We propose that T429 helps initiate strand separation at either position by using its hydroxyl group to compete for hydrogen bonding between the bases at −11 and/or −10, thereby weakening the base pairing between these bases. This would facilitate capture of the base(s) by RNAP to initiate the strand-separation process, a concept that had been proposed earlier by Matlock and Heyduk.[13] Any disruption of base pairing by T429 at both −11 and −10 is likely to be sequential, with the −11 base pair melted first. The exact target of T429 may not be easily elucidated, as it is likely that each DNA base is contacted by multiple amino acid residues and vice versa,[25] forming a network of interactions.

Comparison of T429A RNAP with a σ^{70}-substituted RNAP that forms stable closed complexes

In previously published work,[18,19] we have characterized another RNAP bearing substitutions in region 2.3 of σ^{70}. With four aromatic amino acids in region 2.3 substituted by alanine (F427, Y430, W433, and W434), this form of σ^{70} was designated FYWW. While the footprints of T429A (50 nM RNAP, 0.5 min of incubation) and FYWW (150 nM RNAP, 10 min of incubation) RNAP on the extended long duplex at 9 °C are similar (data not shown), there are fundamental differences in the behaviors of these two enzymes. We have not been able to detect a significant amount of open complex formation by FYWW RNAP under any conditions assayed so far. However, the T429A RNAP characterized here exhibits slow kinetics, but has been found to form open complexes on almost all extended long duplex promoters in solution in 10 min (see Fig. 5). This distinction likely reflects a fundamental difference in the mechanisms by which the substituted amino acid residues participate in strand separation. While T429 would accelerate the initiation of strand separation, the T429A RNAP would retain the ability to carry out the subsequent steps (involving capture of −11A) once −11A has spontaneously rotated out of the DNA helix. On the other hand, the four substitutions in the FYWW σ^{70} are proposed to form the −11A binding pocket on RNAP. This mutated RNAP would then be deficient in holding onto −11A, rendering it unable to form open complexes regardless of the strength of the promoter or the time of incubation. The model presented here is compatible with an active role for RNAP in effecting promoter DNA strand separation, which may also require DNA bending to further weaken the base pairing at −11.[26] The alternative would be a passive role where RNAP would merely capture −11A during a spontaneous excursion out of the DNA helix.

Conclusion

Our data demonstrate that T429 is a key player in the nucleation of promoter DNA melting. The hydroxyl group of the threonine was found to be critical, providing support for a model where it would play a role in disrupting the base pairing of the −11 and/or the −10 base pairs of promoter DNA to facilitate the flipping of −11A out of the helix. Thus, RNAP would play an active role in nucleating the strand-separation step that results in the formation of the open RNAP–promoter complex.

Materials and Methods

Materials

Oligodeoxynucleotides were synthesized by Invitrogen or Integrated DNA Technologies. [γ-^{33}P]ATP was purchased from Perkin Elmer, DNA-modifying enzymes were purchased from either New England Biolabs or Roche, and *E. coli* RNAP core was purchased from EpiCenter. All chemicals were obtained from Sigma, Fisher, or Amresco.

Protein purification, characterization, and reconstitution

E. coli sigma factors were purified using a nondenaturing protocol from Zhi and Jin, with minor modifications, as described.[11,27] The holoenzyme was reconstituted from purified RNAP core (400 nM) and WT or substituted σ^{70} by incubation on ice for 1 h. The amount of σ^{70} added (5- to 15-fold excess over the core enzyme, depending on the particular preparation) was determined in separate assays to give maximal formation of stable complexes with promoter DNA, radiolabeled, and annealed as previously described.[11]

Gel-shift assays for holoenzyme formation

Reconstituted RNAP (7.5 μl) was added to 2.5 μl of 4× native dye solution (125 mM Tris–HCl pH 6.8, 40% glycerol, and 0.01% bromophenol blue). All 10 μl was then loaded onto a Tris–HCl 4–20% PAGE Readygel (BioRad; catalog no. 161-1105) and run at low voltage in a native running buffer (25 mM Tris, 170 mM glycine, and 0.1% SDS pH 8.3). The gel was then rinsed with ddH_2O and stained for 1 h with Gelcode® Blue (Pierce). Documentation of the gel was performed using the Chemi Genius Bio Imaging System (Syngene).

EMSA

These binding assays were carried out as previously described[11] in fork-binding buffer [FBB; 30 mM Hepes pH 7.5, 1 mM dithiothreitol, 0.1 mg/ml bovine serum albumin, 100 mM NaCl, 0.1 mM ethylenediaminetetraacetic acid (EDTA) pH 8, and 1% glycerol]. Generally, 10 nM annealed DNA and 50 nM RNAP holoenzyme were incubated at room temperature (23–26 °C) for 10 min (or 5 min, where indicated). To assay for the formation of stable complexes, reactions were challenged with 200 μg/ml heparin for an additional 10 min (or 5 min, where indicated); for reactions without heparin challenge, 1 μl of ddH_2O was added, and incubation was continued for another 10 min. Four percent nondenaturing gels were loaded and run at room temperature as described; after the gels had been dried, they were analyzed by PhosphorImaging (Molecular Dynamics) using ImageQuant 5.2 software to quantify the radiolabeled free and RNAP-bound DNA. For EMSA experiments performed at 18 °C or 9 °C, an Echo Therm chilling/heating plate (Torrey Pines Scientific) was used to maintain the temperature, and gels were run at the same temperature in a Protean II xi cell electrophoresis unit (BioRad). Here and elsewhere, error was determined from half of the spread of the values (two experiments) or the standard deviation (three or more experiments).

Obtaining association rate constants by EMSA

Experiments for determining k_{obs} were performed essentially as described.[11] Briefly, the binding reaction was initiated by the addition of reconstituted RNAP (final concentration, 50 nM) to 10 nM annealed and radiolabeled DNA in 10 μl of 1×FBB at 18 °C. After the desired incubation times, 1 μl of 2 mg/ml heparin (final concentration, 200 μg/ml) was added for 30 s to dissociate nonspecific and heparin-sensitive specific complexes. Addition of dye and loading were performed as described earlier for EMSA experiments run at 18 °C. Fractions of DNA bound were determined and plotted as a function of time and fit using Kaleidagraph version 3.52 according to the following single-exponential equation: $y = y_{max}(1 - \exp(-k_{obs}t))$, where y_{max} is the amplitude and k_{obs} is the pseudo-first-order rate constant for the association of RNAP and promoter DNA to form a heparin-resistant complex. Experiments for determining the k_{off} values of heparin-resistant complexes were performed in 30-μl reaction mixtures containing the same components as for the association kinetics. After a 10-min incubation at 18 °C, complexes were challenged with 200 μg/ml heparin, and time points were taken thereafter. Addition of dye and gel loading were performed as described earlier.

DNase I footprinting

The end labeling of the 237-bp λ P_R fragment was performed as described.[19] The DNA (~3 nM), ^{33}P labeled at the 5′ end of the template strand, was incubated with 100 nM reconstituted RNAP at room temperature in transcription buffer (30 mM Tris–HCl pH 7.3, 20 mM KCl, 10 mM $MgCl_2$, 0.1 mM EDTA, 50 μg/ml bovine serum albumin, and 10 mM dithiothreitol). The final volume of the reactions was 20 μl. After 10 min of incubation, DNase I was added to a final concentration of 0.01 U/μl, and incubation at room temperature was allowed to proceed for 30 s. For reactions requiring heparin challenge, 1 μl of 2 mg/ml heparin was added, and incubation proceeded for 1 min before the addition of DNase I. Reactions were stopped by the addition of 2 vol of 4 M NH_4Ac, followed by ethanol precipitation in the presence of 80 μg/ml glycogen. Pellets were washed with 70% ethanol, resuspended in formamide dye,[11] and loaded onto a 6% sequencing gel containing 25% formamide. Gels were fixed with 5% acetic acid and 20% methanol, dried, and exposed for 2 days to a PhosphorImaging screen before scanning (Molecular Dynamics).

The extended long duplex promoter DNA was derived from the cloning of the 65-bp annealed long duplex promoter into a pCR-Blunt II-TOPO vector (Invitrogen).

End labeling of the 242-bp extended long duplex was performed by PCR amplification using a nontemplate-sequence primer that was 5′ end labeled with ^{33}P and an unlabeled template-sequence primer. DNase I footprinting experiments using the extended long duplex promoter were performed similarly, except that the FBB used for the EMSA experiments was additionally supplemented with 5 mM $MgCl_2$ (final concentration in the reactions), RNAP concentration was 50 nM, and reactions were incubated at 9 °C for either 0.5 min or 10 min. The volume and incubation time of the DNase I reaction were the same, but DNase I was used at 0.06 U/μl instead, in view of the lower temperature.

DNase I footprinting patterns were analyzed using ImageQuant 5.2. To compare the different reactions, quantified traces for the different lanes were normalized to the same peak (a chosen band that is outside the footprinted region) using Microsoft Excel. To correct for the nonalignment of peaks in different lanes due to uneven running of the gel (only for the graph in Fig. 6b), the bands just upstream of the −48 peak for the No-RNAP lane were shifted to the right, and those for T429A RNAP were shifted to the left to properly align the peaks. The traces shown in Fig. 5b did not require modification of this type.

$KMnO_4$ probing

Reactions contained 10 nM annealed long duplex DNA (5′ end labeled at the nontemplate strand) in Tris-binding buffer (40 mM Tris–HCl pH 8, 40 mM KCl, and 1 mM $MgCl_2$) and were started by the addition of 50 nM RNAP (final volume, 20 μl). Incubation was carried out at 18 °C for 1 min, 10 min, or 60 min, then $KMnO_4$ was added to a final concentration of 2 mM. After 30 s, 5 μl of stop solution containing 1.5 M NaOAc pH 8, 4 mg/ml glycogen, and 300 mM β-mercaptoethanol was added, and reactions were placed on ice. Further work-up was performed exactly as described, except that an 8% sequencing gel was used instead of a 10% gel.[11] To compare the extents of RNAP-induced melting of the long duplex DNA, the −1 and +2T bands were used to quantify the strand opening. The total radioactivity of these bands in each lane was divided by that of full-length DNA, and the values were then normalized to that obtained for WT RNAP after a 60-min incubation.

For reactions performed at 9 °C, the same Tris-binding buffer was used similarly as for the previous $KMnO_4$ experiment, except that the $MgCl_2$ concentration was 5 mM instead of 1 mM in order to make more direct comparisons to the DNase I footprinting experiments. Here, about 3 nM nontemplate strand ^{33}P-labeled 242-bp extended long duplex DNA and 50 nM RNAP were incubated at 9 °C for 0.5 min or 10 min. Heparin was added to a final concentration of 100 μg/ml and incubated for 1 min before the addition of 1 μl of 63 mM $KMnO_4$ (a final concentration of 3 mM due to the lower temperature of the experiment). Additional work-up was performed as described for the protocol earlier, except that a 6% sequencing gel was used for loading the reactions. To quantify strand opening, all four melted bands were used (−10T, −6T, −1T, and +2T).

Structural modeling

The structure presented in Fig. 7 is based on that determined by Murakami *et al.* for the complex of the holoenzyme with a fork-junction DNA template (double stranded to −12; single stranded from −11 to −7 of the nontemplate strand).[23] Starting with the backbone coordinates of Protein Data Bank file 1L9Z,[23] we built and minimized the sigma subunit residues 252–257 (*Thermus aquaticus* numbering) and the nontemplate strand bases in the −12 to −7 region, using CHARMM version 30 with the version 27 parameter set.[28] The figures were made using Visual Molecular Dynamics 1.8.2.[29] To emulate the double-stranded DNA characteristic of a closed complex, using the program 3DNA,[30] an 8-bp canonical B-DNA double helix was modeled in as the template DNA, complementary to the −7 to −14 promoter sequence GCTATACT.[23] The −8 to −11 nontemplate backbone of the B-DNA model was superimposed upon the backbone of the 1L9Z crystal structure. The base positions were similar to those found with CHARMM.

Acknowledgements

We thank Dr. Mark Caprara for critically reading a version of this manuscript and Victoria Cook for generously supplying the nonmelting FYWW RNAP used for some unpublished experiments. This work was supported by National Institutes of Health grant GM 31808 to P.L.dH.

References

1. deHaseth, P. L., Zupancic, M. & Record, M. T., Jr (1998). RNA polymerase–promoter interactions: the comings and goings of RNA polymerase. *J. Bacteriol.* **180**, 3019–3025.
2. Gross, C., Chan, C., Dombroski, A., Gruber, T., Sharp, M., Tupy, J. & Young, B. A. (1998). The functional and regulatory roles of sigma factors in transcription. *Cold Spring Harbor Symposia on Quantitative Biology*, Cold Spring Harbor Laboratory Press, Plainview, NY 63, 141–155.
3. Helmann, J. D. & deHaseth, P. L. (1999). Protein–nucleic acid interactions during open complex formation investigated by systematic alteration of the protein and DNA binding partners. *Biochemistry*, **37**, 5959–5967.
4. Craig, M. L., Tsodikov, O. V., McQuade, K. L., Schlax, P. E., Jr, Capp, M. W., Saecker, R. M. & Record, M. T., Jr (1998). DNA footprints of the two kinetically significant intermediates in formation of an RNA polymerase–promoter open complex: evidence that interactions with the start site and downstream DNA induce sequential conformational changes in polymerase and DNA. *J. Mol. Biol.* **283**, 741–756.
5. Saecker, R. M., Tsodikov, O. V., McQuade, K. L., Schlax, P. E., Capp, M. W. & Record, M. T., Jr (2002). Kinetic studies and structural models of the association of *E. coli* σ^{70} RNA polymerase with the λ P_R promoter: large scale conformational changes in forming the kinetically significant intermediates. *J. Mol. Biol.* **319**, 649–671.
6. Davis, C. A., Bingman, C. A., Landick, R., Record, M. T., Jr & Saecker, R. M. (2007). Real-time footprinting of DNA in the first kinetically significant intermediate in open complex formation by *Escherichia coli* RNA polymerase. *Proc. Natl Acad. Sci. USA*, **104**, 7833–7838.
7. Juang, Y.-L. & Helmann, J. D. (1994). A promoter melting region in the primary sigma factor of *Bacillus*

subtilis: identification of functionally important aromatic amino acids. *J. Mol. Biol.* **235**, 1470–1488.
8. Fenton, M. S., Lee, H. J. & Gralla, J. D. (2000). *Escherichia coli* promoter opening and −10 recognition: mutational analysis of σ^{70}. *EMBO J.* **19**, 1130–1137.
9. Tomsic, M., Tsujikawa, L., Panaghie, G., Wang, Y., Azok, J. & deHaseth, P. L. (2001). Different roles for basic and aromatic amino acids in conserved region 2 of *Escherichia coli* σ^{70} in the nucleation and maintenance of the single-stranded DNA bubble in open RNA polymerase–promoter complexes. *J. Biol. Chem.* **276**, 31891–31896.
10. Panaghie, G., Aiyar, S. E., Bobb, K. L., Hayward, R. S. & deHaseth, P. L. (2000). Aromatic amino acids in region 2.3 of *Escherichia coli* sigma 70 participate collectively in the formation of an RNA polymerase–promoter open complex. *J. Mol. Biol.* **299**, 1217–1230.
11. Schroeder, L. A., Choi, A.-J. & deHaseth, P. L. (2007). The −11A of promoter DNA and two conserved amino acids in the melting region of σ^{70} both directly affect the rate limiting step in formation of the stable RNA polymerase–promoter complex, but they do not necessarily interact. *Nucleic Acids Res.* **35**, 4141–4153.
12. Waldburger, C. & Susskind, M. M. (1994). Probing the informational content of *Escherichia coli* sigma 70 region 2.3 by combinatorial cassette mutagenesis. *J. Mol. Biol.* **235**, 1489–1500.
13. Matlock, D. L. & Heyduk, T. (2000). Sequence determinants for the recognition of the fork junction DNA containing the −10 region of promoter DNA by *E. coli* RNA polymerase. *Biochemistry*, **39**, 12274–12283.
14. Heyduk, E., Kuznedelov, K., Severinov, K. & Heyduk, T. (2006). A consensus adenine at position −11 of the nontemplate strand of bacterial promoter is important for nucleation of promoter melting. *J. Biol. Chem.* **281**, 12362–12369.
15. Schroeder, L. A. & deHaseth, P. L. (2005). Mechanistic differences in promoter DNA melting by *Thermus aquaticus* and *Escherichia coli* RNA polymerases. *J. Biol. Chem.* **280**, 17422–17429.
16. Lim, H. M., Lee, H. J., Roy, S. & Adhya, S. (2001). A "master" in base unpairing during isomerization of a promoter upon RNA polymerase binding. *Proc. Natl Acad. Sci USA*, **98**, 14849–14852.
17. Tsujikawa, L., Strainic, M. G., Watrob, H., Barkley, M. D. & deHaseth, P. L. (2002). RNA polymerase alters the mobility of an A-residue crucial to polymerase-induced melting of promoter DNA. *Biochemistry*, **41**, 15334–15341.
18. Sun, L., Dove, S., Panaghie, G., deHaseth, P. L. & Hochschild, A. (2004). An RNA polymerase mutant deficient in DNA melting facilitates study of activation mechanism: application to an artificial activator of transcription. *J. Mol. Biol.* **343**, 1171–1182.
19. Cook, V. M. & deHaseth, P. L. (2007). Strand opening-deficient *E. coli* RNA polymerase facilitates investigation of closed complexes with promoter DNA: effects of DNA sequence and temperature. *J. Biol. Chem.* **282**, 21319–21326.
20. Fenton, M. S. & Gralla, J. D. (2001). Function of the bacterial TATAAT −10 element as single-stranded DNA during RNA polymerase isomerization. *Proc. Natl Acad. Sci. USA*, **98**, 9020–9025.
21. Fenton, M. S. & Gralla, J. D. (2003). Effect of DNA bases and backbone on σ^{70} holoenzyme binding and isomerization using fork junction probes. *Nucleic Acids Res.* **31**, 2745–2750.
22. Lee, H. J., Lim, H. M. & Adhya, S. (2004). An unsubstituted C2 hydrogen of Adenine is critical and sufficient at the −11 position of a promoter to signal base pair deformation. *J. Biol. Chem.* **279**, 16899–16902.
23. Murakami, K. S., Masuda, S., Campbell, E. A., Muzzin, O. & Darst, S. A. (2002). Structural basis of transcription initiation: an RNA polymerase holoenzyme–DNA complex. *Science*, **296**, 1285–1290.
24. Waldburger, C., Gardella, T., Wong, R. & Susskind, M. M. (1990). Changes in conserved region 2 of *Escherichia coli* sigma 70 affecting promoter recognition. *J. Mol. Biol.* **215**, 267–276.
25. Jen-Jacobson, L. (1997). Protein–DNA recognition complexes: conservation of structure and binding energy in the transition state. *Biopolymers*, **44**, 153–180.
26. deHaseth, P. L. & Nilsen, T. W. (2004). When a part is as good as the whole. *Science*, **303**, 1307–1308.
27. Zhi, H. & Jin, D. J. (2003). Purification of highly-active and soluble *Escherichia coli* σ^{70} polypeptide overproduced at low temperature. *Methods Enzymol.* **370**, 174–180.
28. Brooks, B. R., Bruccoleri, R. E., Olafson, B. D., States, D. J., Swaminathan, S. & Karplus, M. (1983). CHARMM: a program for macromolecular energy, minimization, and dynamics calculations. *J. Comput. Chem.* **4**, 187–217.
29. Humphrey, W., Dalke, A. & Schulten, K. (1996). VMD—Visual Molecular Dynamics. *Graphics*, **14**, 33–38.
30. Lu, X.-J. & Olson, W. K. (2003). 3DNA: a software package for the analysis, rebuilding and visualization of three-dimensional nucleic acid structures. *Nucleic Acids Res.* **31**, 5108–5121.